Sigma J Eng & Nat Sci 37 (3), 2019, 1031-1053

Sigma Journal of Engineering and Natural Sciences
Sigma Mühendislik ve Fen Bilimleri Dergisi

Research Article

HEAT AND MASS TRANSFER IN MAGNETOHYDRODYNAMICS (MHD) FLOW OVER A MOVING VERTICAL PLATE WITH CONVECTIVE BOUNDARY CONDITION IN THE PRESENCE OF THERMAL RADIATION

B. Johnson AKINBO*[1], Bakai I. OLAJUWON[2]

[1]*Department of Mathematics, Federal University of Agriculture, Abeokuta, NIGERIA;*
ORCID: 0000-0003-3200-6266
[2]*Department of Mathematics, Federal University of Agriculture, Abeokuta, NIGERIA;*
ORCID: 0000-0002-6269-7929

Received: 27.11.2018 Revised: 12.06.2019 Accepted: 29.07.2019

ABSTRACT

This paper investigates heat and mass transfer in a Magnetohydrodynamic flow over a moving vertical plate with convective boundary condition in the presence of thermal radiation. Similarity method is used to transform the system of coupled non-linear partial differential equations, governing the flow, heat and mass transfer problems to a system of coupled non-linear ordinary differential equations. The resulting equation is then solved, using Homotopy Analysis Method (HAM). The effect of thermal radiation, Magnetic Parameter and all other parameters encountered in the course of the investigation were examined on the fluid flow, heat and mass transfer. The results show among all other obtained that higher values of radiation parameter pioneer the dominance of conduction over radiation and consequently depressed the thermal boundary layer thickness.
Keywords: Vertical plate, similarity solution, magnetic field, thermal radiation, heat and mass transfer, homotopy analysis method (HAM).

1. INTRODUCTION

In most of the practical transport processes, the heat transfer is always accompanied by the mass transfer. The study of magnetohydrodynamic (MHD) flow with heat and Mass transfer over a moving surface and the effect of thermal radiation has been of interest due to its wide application scientific and environmental process such as astrophysical flows and geothermal reservoir. As a result of the various application of this problem, it has attracted the attention of many researchers and extensively studied in the literature.

* Corresponding Author: e-mail: akinbomaths@gmail.com

Nomenclatures

g	$Acceleration\ due\ to\ gravity$	α	$Thermal\ diffusivity$
D	$Mass\ diffusivity$	β_T	$Thermal\ expansion\ coeficient$
(x, y)	$Coordinates$	v	$Kinematic\ viscosity$
η	$Similarity\ variable$	ρ	$Fliud\ density$
ψ	$Stream\ function$	β_c	$Concentration\ expansion\ Coefficient$
μ	$Dynamic\ viscosity$		

Das (2010) and Seethamahalakshmi et'al. (2011) studied MHD free convection flow and Mass transfer near a moving vertical plate in the presence of thermal radiation. Their results showed that increase in thermal radiation parameter contributes to the decrease in velocity field. Ghara et'al (2012) reported the effect of radiation on MHD free convection flow past an impulsively moving vertical plate with ramped wall temperature, buttressed by Siva et'al (2016). It was reviewed that temperature profile increases the increase in thermal radiation and Eckert number. The radiation effect on the flow past a vertical plate with the mass transfer was examined by Rajput and Kumar (2012). Narahari and Ishaq (2011) reported the radiation effects of free convection flow near a moving vertical plate with Newtonian heating. Das et'al. (2015) and Nepal et'al. (2014) observed the free convection flo w past a vertical plate with heat and mass fluxes in the presence of thermal radiation and concluded that thermal boundary layer thickness increases with increase in radiation parameter. Attention has also been given to the hall effect as Mohammed et'al (2013) observed the heat and Mass transfer in MHD free convection flow over an inclined plate with hall current and reported that there is no effect of the Magnetic parameter and Schmidt number on the temperature field and concentration. However, Gnaneswara (2014) reported the effect of the hall parameter in the temperature is small and the magnetic and hall parameters have opposite effects on the velocity and temperature profiles while studying the effect of thermal radiation, viscous dissipation and hall current effects in the MHD convection flow over a stretched vertical flat plate.

Several investigations were performed on porosity in a medium with different conditions. Sandeep et'al (2012), Salem and Rania (2012) studied MHD heat and mass transfer through a porous medium as well as Jhansi et al (2015). Other authors like Idowu et'al (2013), Lakshmi et'al. (2014) and Olubode et'al (2016) investigated MHD flow along a vertical porous plate. Recently, Opiyo and Alfred (2017) studied the effects of Magnetohydrodynamic (MHD) fluid flow on a two-dimension boundary layer flow of a steady free convection heat and Mass transfer in an inclined plane in which the angle of inclination is varied. It was found that the velocity increases with an increase in the thermal and Solutal Grashof numbers. The velocity and concentration of the fluid decrease with an increase in the Schmidt number.

The objective of this present investigation is to extend the work in Makinde (2010) to include Heat and Mass transfer in Magnetohydrodynamic (MHD) flow over a moving vertical plate with convective boundary condition in the presence of thermal radiation. The governing equations are solved analytically via Homotopy Analysis Method (HAM), developed by Liao (2003) and effect of different Parameters on fluid flow are considered.

2. MATHEMATICAL FORMULATION

Consider a steady-state two-dimensional boundary layer flow of a stream of cold incompressible electrically conducting fluid along a vertical plate. The surface of the plate is assumed to be heated by convection from a hot fluid at temperature T_f that produces a heat transfer coefficient h_f. The cold fluid in contact with the surface of the plate generate heat internally at volumetric rate Q_0. A magnetic field B_0 is placed in a transverse direction to the flow. The magnetic Reynolds number is assumed to be small therefore the induced magnetic field is neglected. The joule heating term in energy equation is assumed to be neglected as it really

very small in slow motion free convection flow. $x-axis$ is taken parallel to the plate direction and $y-axis$ normal to it (see fig.1). C_w is the species concentration while T_∞ and C_∞ represent ambient temperature and concentration respectively. The fluid velocities in x and y dircetions are denoted by u and v respectively. The fluid temperature and concentration are respectively taken as T and C.

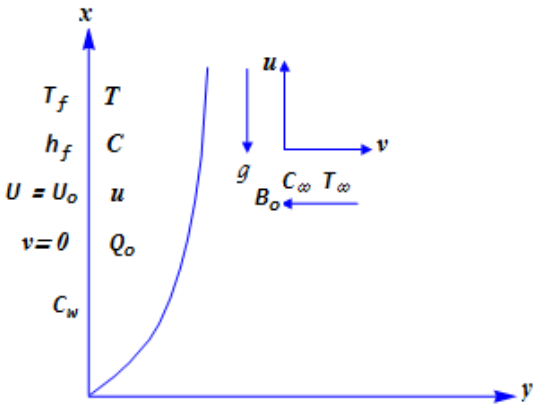

Figure 1. Flow configuration and coordinate system

Under the assumption stated above, boundary layer approximation and usual Boussinesq's approximation, the governing equations the present problem can be expressed as

$$\frac{\partial u}{\partial x}+\frac{\partial v}{\partial y}=0 \tag{1}$$

$$u\frac{\partial u}{\partial x}+v\frac{\partial u}{\partial y}=\nu\frac{\partial^2 u}{\partial y^2}-\frac{\sigma B_0 u}{\rho}+g\,\beta_T(T-T_\infty)+g\,\beta_c(C-C_\infty) \tag{2}$$

$$u\frac{\partial T}{\partial x}+v\frac{\partial T}{\partial y}=\alpha\frac{\partial^2 T}{\partial y^2}+\frac{\nu}{C_p}\left(\frac{\partial u}{\partial y}\right)^2-\frac{1}{\rho C_p}\frac{\partial q_r}{\partial y}+\frac{Q_0(T-T_\infty)}{\rho C_p} \tag{3}$$

$$u\frac{\partial C}{\partial x}+v\frac{\partial C}{\partial y}=D\frac{\partial^2 C}{\partial y^2} \tag{4}$$

with the following boundary conditions

$$U(x,0)=U_0,\ V(x,0)=0,\ -k\frac{\partial T(x,0)}{\partial y}=h_f[T_f-T(x,0)],\ C_w(x,0)=Ax^\lambda+C_\infty$$
$$U(x,\infty)=0,\ T(x,\infty)=T_\infty,\ C(x,\infty)=C_\infty \tag{5}$$

where λ denotes the power index of the concentration and k is the thermal conductivity coefficient.

The radiative heat flux by Roseland is adopted and expressed as

$$q_r=\frac{-4\sigma}{3K^*}\frac{\partial T^4}{\partial y} \tag{6}$$

where σ is the Sterfan-Boltzmann constant and K^* is the mean of absorption coefficient. It is assumed that the temperature differences within the flow are such that the term T^4 can be expressed as a linear function of temperature by expanding T^4 in a Taylor series about T_∞ as;

$$T^4=T_\infty^4T+4T_\infty^3(T-T_\infty)-6T_\infty^2(T-T_\infty)^2+\ldots \tag{7}$$

and neglecting higher order terms beyond the first degree in $(T-T_\infty)$ gives

$$T^4\approx 4T_\infty^3T-3T_\infty^4 \tag{8}$$

The substitution of equations (6) and (8) in equation (3) gives a modified equation of the form

$$u\frac{\partial T}{\partial x}+v\frac{\partial T}{\partial y}=\alpha\frac{\partial^2 T}{\partial y^2}+\frac{v}{C_p}\left(\frac{\partial u}{\partial y}\right)^2+\frac{16\sigma T_\infty}{3K^*\rho C_p}\frac{\partial^2 T}{\partial y^2}+\frac{Q_0(T-T_\infty)}{\rho C_p} \tag{9}$$

Following Makinde (2010) and Mohammed et'.al (2015), the continuity equation (1) is satisfied automatically by invoking the stream function defined by

$$u=\frac{\partial\psi}{\partial y}\quad and\quad v=-\frac{\partial\psi}{\partial x} \tag{10}$$

and obtained similarity equations of the problem by introducing the following similarity transformation

$$\eta=y\sqrt{\frac{U_0}{vx}},\ \ \psi=\sqrt{vxU_0}f(\eta),\ \ \theta(\eta)=\frac{T-T_\infty}{T_f-T_\infty},\ \ \emptyset(\eta)=\frac{C-C_\infty}{C_w-C_\infty} \tag{11}$$

Where η is an independent similarity variable, $\theta(\eta)$ and $\emptyset(\eta)$ are dimensionaless temperature and concentration respectively, U_0 is the velocity of the plate. Apply equation equations (10) and (11) into equations (2), modified equation (9) and equation (4), we have

$$f'''(\eta)+\frac{1}{2}f(\eta)f''(\eta)-Haf'(\eta)+Gr\theta(\eta)+Gc\emptyset(\eta)=0 \tag{12}$$

$$\left(1+\frac{4}{3R_a}\right)\theta''(\eta)+PrEc(f''(\eta))^2+\frac{1}{2}Pr\theta'(\eta)f(\eta)+Q\theta(\eta)=0 \tag{13}$$

$$\emptyset''(\eta)+\frac{1}{2}Scf(\eta)\emptyset'(\eta)=0 \tag{14}$$

Which agreed with Makinde (2010), Rout et'al (2013), Lakshmi et'al.(2014), Hemalatha and Bhaskar (2015) where the prime symbol represents differentiation with respect to η and

$$Ha=\frac{\sigma B_0^2 x}{\rho U_0},\quad Gr=\frac{g\beta_T(T_f-T_\infty)x}{U_0^2},\quad Gc=\frac{g\beta_c(C_w-C_\infty)x}{U_0^2},\quad Bi=\frac{hf}{k}\sqrt{\frac{vx}{U_0}},$$
$$Pr=\frac{v}{\alpha},\quad Sc=\frac{v}{D},\quad Q=\frac{xQ_0v}{k^*U_0},\ Ec=\frac{U_0^2}{C_p(T_f-T_\infty)},Ra=\frac{4\sigma T_\infty}{KK^*},\ \alpha=\frac{k^*}{\rho C_\rho} \tag{15}$$

For Ha is the local magnetic field parameter, Gr is the local thermal Grashof number, Gc is the Solutal Grashof number, Bi is the local convective heat transfer parameter, Pr is the Prandtl number, Sc is the Schmidt number, Q is the heat source, Ec is the Eckert number and Ra is the Radiation parameter. The corresponding boundary conditions are as follows

$$f(0)=0,\ f'(0)=1,\ \theta'(0)=Bi[\theta(0)-1],\ \emptyset(0)=1 \tag{16}$$

$$f'(\infty)=0,\ \theta(\infty)=0,\ \ \emptyset(\infty)=0 \tag{17}$$

The local parameters Bi, Ha, Gr, Q and Gc in (12-14) denotes the function of x. In an attempt to have similarity solution, we assume the following parameters

$$h_f=\frac{p}{\sqrt{x}},\quad \sigma=\frac{q}{x},\quad \beta_T=\frac{r}{x},\quad \beta_T=\frac{s}{x},\quad Q_0=\frac{t}{x} \tag{18}$$

Where $p,q,r,x,$ and t are constant under the appropriate dimension. The coupled equations (12-14) subject to the boundary conditions of equations (16) and (17) are solved analytically by Homotopy Analysis Method as shown in (3.0) below. For the purpose of Engineering application, we compute the local skin friction coefficient, the Local Nusselt number, the Local Sherwood number and the plate surface temperature are considered interms of $f''(0),-\theta'(0),-\emptyset'(0)$ and $\theta(0)$ respectively and the results obtained are presented in the tabular form.

3. HOMOTOPY ANALYSIS METHOD

The set of coupled Non-linear differential equations are usually inevitable and has become a culture in mathematical modeling. They are solved by a different method, among which are;

Adomian Decomposition, Variation Iteration Method and so on. Homotopy Analysis Method (HAM), discovered by Liao (2003) was preferred over another method due to its efficiency in solving both Linear and non-linear differential equation particularly at infinite domain. We consider the differential equations

$$L[f(\eta)] = 0 \quad and \quad N[f(\eta)] = 0 \tag{19}$$

where L and N are called Linear and non-linear function respectively (for Algebra Equation) or Linear and Non-linear operator respectively (for differential Equations), η represents an independent variable, while $f(\eta)$ is the solution of (19).

Let $f_0(\eta)$ be initial guess for $f(\eta)$ and $\hbar \neq 0$, $H(\eta) \neq 0$ denote the auxillary parameter, auxiliary function respectively, we then construct a family equation of the form

$$(1-r)L[f(\eta;r) - f_0(\eta)] = r\hbar H(\eta)N[f(\eta;r)] \tag{20}$$

where $r \in [0,1]$ is called an embedding parameter. When, $r = 0$, we have

$$f(\eta;0) = f_0(\eta) \quad and \quad N[f(\eta;1)] = 0 \; but \; \hbar H(\eta) \neq 0 \quad for, \; r = 1 \tag{21}$$

Hence, in respect to the boundary conditions (16) and (17), $f(\eta), \theta(\eta)$ and $\emptyset(\eta)$
Can be expressed by the set of base functions

$$\{ \eta^j \exp(-nj) \mid j \geq 0, n \geq 0 \} \tag{23}$$

in the following form

$$f(\eta) = \sum_{n=0}^{\infty}\sum_{k=0}^{\infty} a_{n,k}^k \eta^k \exp(-nj), \; \theta(\eta) = \sum_{n=0}^{\infty}\sum_{k=0}^{\infty} b_{n,k}^k \eta^k \exp(-nj) \; and \; \emptyset(\eta) = \sum_{n=0}^{\infty}\sum_{k=0}^{\infty} c_{n,k}^k \eta^k \exp(-nj) \tag{24}$$

where $a_{n,k}^k$, $b_{n,k}^k$ and $c_{n,k}^k$ are coefficients. However, as long as such a set of base functions is determined, the auxiliary function $H(\eta)$, initial approximation $f_0(\eta)$, $\theta_0(\eta)$, $\emptyset_0(\eta)$, and the auxiliary linear operators L_f, L_θ, and $L_\emptyset$ must be chosen in such a way that solution of the corresponding high-order deformation exist (see Farooq et'al (2015) and Olubode et'al (2016)). The point raised above is essential in the framework of homotopy Analysis Method as its provide us with a basic rule called the rule of solution expression for $f(\eta), \theta(\eta)$ and $\emptyset(\eta)$. In accordance with the rule of solution and boundary conditions (16) – (17), we choose the initial guess

$$f_0(\eta) = 1 - exp(-\eta), \quad \theta_0(\eta) = \frac{Bi\, exp(-\eta)}{(1+Bi)}, \quad \emptyset_0(\eta) = exp(-\eta) \tag{25}$$

as the initial linear approximations of $f(\eta), \theta(\eta)$ and $\emptyset(\eta)$. The auxiliary linear operations L_f, L_θ, and $L_\emptyset$ are;

$$L_f[f(\eta;r)] = \frac{\partial^3 f(\eta;r)}{\partial \eta^3} - \frac{\partial f(\eta;r)}{\partial \eta}, L_\theta[\theta(\eta;r)] = \frac{\partial^2 \theta(\eta;r)}{\partial \eta^2} - \theta(\eta;r) \; and \; L_\emptyset[(\eta;r)] = \frac{\partial^2 \emptyset(\eta;r)}{\partial \eta^2} - \emptyset(\eta;r) \tag{26}$$

agreed with the following properties

$$L_f[C_1 + C_2\, exp(\eta) + C_3\, exp(-\eta)] = 0, \; L_\theta[C_4 + C_5\, exp(-\eta)] = 0 \; and \; L_\emptyset[C_6 + C_7\, exp(-\eta)] = 0 \tag{27}$$

where $C_1, C_2, \ldots, C_7$ are constants.

3.1. Zero Order Deformation Problem.

$$(1-r)L_f[f(\eta;r) - f_0(\eta)] = r\hbar_f H_f(\eta)N_f[f(\eta;r), \theta(\eta;r), \emptyset(\eta;r)] \tag{28}$$

$$(1-r)L_\theta[f(\eta;r) - \theta_0(\eta)] = r\hbar_\theta H_\theta(\eta)N_\theta[f(\eta;r), \theta(\eta;r)] \tag{29}$$

$$(1-r)L_\emptyset[f(\eta;r) - \emptyset_0(\eta)] = r\hbar_\emptyset H_\emptyset(\eta)N_\emptyset[f(\eta;r), \emptyset(\eta;r)] \tag{30}$$

having the following boundary conditions.

$$f(\eta=0;r)=0,\ \frac{\partial f(\eta;r)}{\partial \eta}\Big|_{\eta=0}=1,\quad \frac{\partial \theta(\eta;r)}{\partial \eta}\Big|_{\eta=0}=Bi[\theta(\eta=0;r)-1],\emptyset(\eta=0;r)=1 \tag{31}$$

$$\frac{\partial f(\eta;r)}{\partial \eta}\Big|_{\eta\to\infty}=0,\ \theta(\eta\to\infty;r)=0=\emptyset(\eta\to\infty;r) \tag{32}$$

The nonlinear operator followed from equations (12)-(14) and defined as

$$\frac{\partial^3 f(\eta;r)}{\partial \eta^3}+\frac{1}{2}f(\eta;r)\frac{\partial^2 f(\eta;r)}{\partial \eta^2}-Ha\frac{\partial f(\eta;r)}{\partial \eta}+Gr\theta(\eta;r)+Gc\emptyset(\eta;r)=0 \tag{33}$$

$$\left[1+\frac{4}{3R_a}\right]\frac{\partial^2 \theta(\eta;r)}{\partial \eta^2}+PrEc\left(\frac{\partial^2 f(\eta;r)}{\partial \eta^2}\right)^2+\frac{1}{2}Pr\frac{\partial \theta(\eta;r)}{\partial \eta}f(\eta;r)+Q\theta(\eta;r)=0 \tag{34}$$

$$\frac{\partial^2 \emptyset(\eta;r)}{\partial \eta^2}+\frac{1}{2}Scf(\eta;r)\frac{\partial \emptyset(\eta;r)}{\partial \eta}=0 \tag{35}$$

where $r\epsilon[0,1]$ is the same as embedding parameter defined above. Putting $r=0$ and $r=1$, we respectively have the following solution from equation (28)-(30).

$$L_f[f(\eta;0)-f_0(\eta)]=0,\ L_\theta[\theta(\eta;0)-\theta_0(\eta)]=0,\ L_\emptyset[\emptyset(\eta;0)-\emptyset_0(\eta)]=0 \tag{36}$$

$$f(\eta;0)=f_0(\eta),\ \theta(\eta;0)=\theta_0(\eta),\quad \emptyset(\eta;0)=\emptyset_0(\eta) \tag{37}$$

With

$$f(\eta=0;0)=0,\frac{\partial f(\eta=0;0)}{\partial \eta}=1,\quad \frac{\partial \theta(\eta=0;0)}{\partial \eta}=Bi[\theta(\eta=0;0)-1],\emptyset(\eta=0;0)=1 \tag{38}$$

$$\frac{\partial f(\eta\to\infty;0)}{\partial \eta}=0,\ \theta(\eta\to\infty;0)=0=\emptyset(\eta\to\infty;0) \tag{39}$$

and

$$0=N_f[f(\eta;r),\theta(\eta;r),\emptyset(\eta;r)],\quad 0=N_\theta[f(\eta;r),\theta(\eta;r)],\quad 0=N_\emptyset[f(\eta;r),\emptyset(\eta;r)] \tag{40}$$

But $\hbar_f H_f(\eta)\neq 0,\hbar_\theta H_\theta(\eta)\neq 0\ and\ \hbar_\emptyset H_\emptyset(\eta)\neq 0$

$$f(\eta;1)=f(\eta),\ \theta(\eta;1)=\theta(\eta),\quad \emptyset(\eta;1)=\emptyset(\eta) \tag{41}$$

with

$$f(\eta=0;1)=0,\ \frac{\partial f(\eta=0;1)}{\partial \eta}=1,\quad \frac{\partial \theta(\eta=0;1)}{\partial \eta}=Bi[\theta(\eta=0;r)-1],\emptyset(\eta=0;1)=1 \tag{42}$$

$$\frac{\partial f(\eta\to\infty;1)}{\partial \eta}=0,\ \theta(\eta\to\infty;1)=0=\emptyset(\eta\to\infty;1) \tag{43}$$

3.2. Mth-Order Deformation Problem

The increase in embedding parameter r from Zero to One$(0-1)$, lead to a variation of the function $f(\eta;r),\theta(\eta;r)$ and $\emptyset(\eta;r)$ from initial guess $f_0(\eta),\ \theta_0(\eta)\ and\ \emptyset_0(\eta)$ to the solutions $f(\eta;r),\theta(\eta;r)$ and $\emptyset(\eta;r)$. Using Taylor series with respect to r, we have

$$f(\eta;r)=f_0(\eta)+\sum_{m=1}^{\infty}f_m(\eta)r^m\ ,\theta(\eta;r)=\theta_0(\eta)+\sum_{m=1}^{\infty}\theta_m(\eta)r^m\ \ and\ \ \emptyset(\eta;r)=\emptyset_0(\eta)+\sum_{m=1}^{\infty}\emptyset_m(\eta)r^m \tag{44}$$

where $\quad f_m(\eta)=\frac{1}{m!}\frac{\partial^m f(\eta;r)}{\partial \eta^m},\ \ f_m(\eta)=\frac{1}{m!}\frac{\partial^m \theta(\eta;r)}{\partial \theta^m},\quad f_m(\eta)=\frac{1}{m!}\frac{\partial^m \emptyset(\eta;r)}{\partial \emptyset^m},$

Obviously, the convergence of the series (44) are subject to the auxiliary parameter $\hbar$. Assuming $\hbar$ is chosen such that the series (44) converge at $r=1$, we have

$$f(\eta)=f_0(\eta)+\sum_{m=1}^{\infty}f_m(\eta),\ \theta(\eta)=\theta_0(\eta)+\sum_{m=1}^{\infty}\theta_m(\eta)\ \ and\quad \emptyset(\eta)=\emptyset_0(\eta)+\sum_{m=1}^{\infty}\emptyset_m(\eta) \tag{45}$$

For the mth-order deformation, we take the derivative of zeroth-order deformation of equations (28)-(30) mtimes with respect to r, dividing by $m!$ and set $r = 0$, we have

$$L_f[f_m(\eta) - \chi_m f_{m-1}(\eta)] = \hbar R_m^f(\eta), L_\theta[\theta_m(\eta) - \chi_m \theta_{m-1}(\eta)] = \hbar R_m^\theta(\eta) \; and \; L_\emptyset[\emptyset_m(\eta) - \chi_m \emptyset_{m-1}(\eta)] = \hbar R_m^\emptyset(\eta) \quad (46)$$

having the following boundary conditions.

$$f_m(\eta = 0; 0) = 0, \frac{\partial f_m(\eta=0;0)}{\partial \eta} = 0, \frac{\partial \theta_m(\eta=0;0)}{\partial \eta} = Bi[\theta_m(\eta = 0; 0)], \emptyset_m(\eta = 0; 0) = 0 \quad (47)$$

$$\frac{\partial f_m(\eta\to\infty)}{\partial \eta} = 0, \; \theta_m(\eta \to \infty) = 0 = \emptyset_m(\eta \to \infty) \quad (48)$$

Where

$$R_m^f(\eta) = \frac{d^3 f_{m-1}(\eta)}{d\eta^3} + \frac{1}{2}\sum_{n=0}^{m-1} f_n(\eta) \frac{d^2 f_{m-1-n}(\eta)}{d\eta^2} - Ha \frac{df_{m-1}(\eta)}{d\eta} + Gr\theta_{m-1} + Gc\emptyset_{m-1} \quad (49)$$

$$R_m^\theta(\eta) = \left[1 + \frac{4}{3R_a}\right] \frac{d^2\theta_{m-1}(\eta)}{d\eta^2} + PrEc \sum_{n=0}^{m-1} \frac{d^2 f_n(\eta)}{d\eta^2} \frac{d^2 f_{m-1-n}(\eta)}{d\eta^2} + \frac{1}{2} Pr \sum_{n=0}^{m-1} f_n(\eta) \frac{d\theta_{m-1-n}(\eta)}{d\eta} + Q\theta_{m-1} \quad (50)$$

$$R_m^\emptyset(\eta) = \frac{d^2\emptyset_{m-1}(\eta)}{d\eta^2} + \frac{1}{2} Sc \sum_{n=0}^{m-1} f_n(\eta) \frac{d\emptyset_{m-1-n}(\eta)}{d\eta} \quad (51)$$

and $\chi_m = 0 \;\; for \;\; m \le 1, \quad \chi_m = 1 \;\; for \;\; m > 1$

having the following as a general solution

$$f_m(\eta) = f_m^*(\eta) + C_1 + C_2 \, exp(-\eta) + C_3 \, exp(\eta) \quad (52)$$

$$\theta_m(\eta) = \theta_m^*(\eta) + C_4 + C_5 \, exp(\eta) \quad (53)$$

$$\emptyset_m(\eta) = \emptyset_m^*(\eta) + C_6 + C_7 \, exp(\eta) \quad (54)$$

where $f_m^*(\eta), \theta_m^*(\eta)$ and $\emptyset_m^*(\eta)$ represent the particular solution of equations (47) and (48). In agreement with Liao (2003), we consider the rule of coefficient ergodicity and rule of solution existence and choose the auxiliary functions as

$$H_f = H_\theta = H_\emptyset = 1$$

3.3. Convergence of the HAM Solution

The convergence of solution of this present investigation as revealed by Liao (2003) is considered, Equation (45) contains the non-zero auxiliary parameters $\hbar_f, \hbar_\theta \; and \; \hbar_\emptyset$ that determine the convergence region and rate of approximation for Homotopy Analysis Method at 10-order with $Ha = 0.1$, $Gr = 0.1$, $Gc = 0.1$, $Pr = 0.72$, $Sc = 0.62$, $Bi = 0.1$, $Q = 0.01$, $Ec = 0.1$, $Ra = 0.7$. The admissible values of $\hbar_f, \hbar_\theta \; and \; \hbar_\emptyset$ was consider at the range where $\hbar - curve$ becomes parallel and resulted in $-1.2 \le \hbar_f \le -03$, $-0.1 \le \hbar_\theta \le 0.2 \; and \; -1.7 \le \hbar_\emptyset \le -0.5$ for $\hbar_f, \hbar_\theta$ and $\hbar_\emptyset$ respectively as shown in figures 2-below

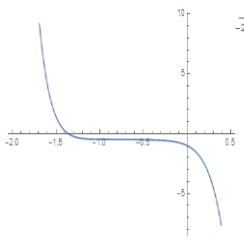

Figure 2. $\hbar_f$-curve of $f''(0)$ at 10th order of approximation

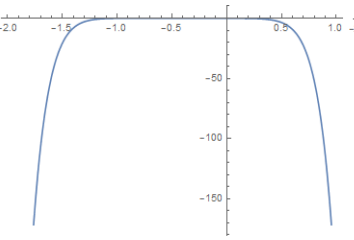

Figure 3. $\hbar_\theta$-curve of $\theta'(0)$ at 10th order approximation

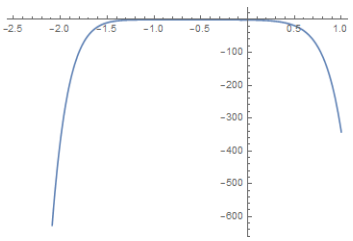

Figure 4. $\hbar_f$-curve of $\emptyset'(0)$ at 10th order of approximation

4. VALIDATION OF THE STUDY

Table 1. Comparison of the present result with Makinde (2010)

						Makinde (2010)				Present result			
Ha	Gr	Gc	Bi	Pr	Sc	$f''(0)$	$-\theta'(0)$	$\theta(0)$	$-\emptyset'(0)$	$f''(0)$	$-\theta'(0)$	$\theta(0)$	$-\emptyset'(0)$
0.1	0.1	0.1	0.1	0.72	0.62	−0.402271	0.078635	0.213643	0.3337425	−0.402272	0.078636	0.213644	0.3337425
1.0	0.1	0.1	0.1	0.72	0.62	−0.352136	0.273153	0.726846	0.3410294	−0.352137	0.273154	0.726845	0.3410295
10	0.1	0.1	0.1	0.72	0.62	−0.329568	0.365258	0.963474	0.3441377	−0.329568	0.365259	0.963475	0.3441377
0.1	0.5	0.1	0.1	0.72	0.62	−0.322212	0.079173	0.208264	0.3451301	−0.322213	0.079174	0.208264	0.3451302
0.1	1.0	0.1	0.1	0.72	0.62	−0.231251	0.079691	0.203088	0.3566654	−0.231252	0.079692	0.203089	0.3566654
0.1	0.1	0.5	0.1	0.72	0.62	−0.026410	0.080711	0.192889	0.3813954	−0.026411	0.080712	0.192889	0.3813955
0.1	0.1	1.0	0.1	0.72	0.62	0.3799184	0.082040	0.179592	0.4176697	0.3799185	0.082041	0.179593	0.4176698
0.1	0.1	0.1	1.0	0.72	0.62	−0.985719	0.074174	0.258252	0.2598499	−0.985720	0.074175	0.258253	0.2598500
0.1	0.1	0.1	5.0	0.72	0.62	−2.217928	0.066156	0.338435	0.1806634	−2.217929	0.066157	0.338436	0.1806634
0.1	0.1	0.1	0.1	1.00	0.62	−0.407908	0.081935	0.180640	0.3325180	−0.407909	0.081936	0.180640	0.3325180
0.1	0.1	0.1	0.1	7.10	0.62	−0.421228	0.093348	0.066513	0.3305618	−0.421229	0.093349	0.066514	0.3305619
0.1	0.1	0.1	0.1	0.72	0.78	−0.411704	0.078484	0.215159	0.3844559	−0.411705	0.078485	0.215160	0.3844560

Here, we first ensure the successful implementation of the numerical result by comparing it with the previous work done. So, these present results are compared to those obtained by Makinde (2010) for the local skin-friction, Nusselt Number, Sherwood number and plate surface temperature by setting $Q = 0,\ Ra = 0,\ Ec = 0$. The results strongly agreed with each other (see Table 1).

5. DISCUSSION OF RESULTS

In order to get a physical understanding of the present problem, equation (12)-(14) with the boundary conditions (16) and (17) have been solved using Homotopy Analysis Method (HAM) at 20th –order to meet the far field boundary condition at infinite domain. The resulting effects of various parameters embedded in the flow system such as; Magnetic Parameter (Ha), Thermal Grashof Number (Gr), Solutal Grashof Number (Gc), Prandtl Number $(Pr.)$, Schmidt Number (Sc), Local Heat transfer parameter (Bi), Heat Source Parameter (Q), Eckert number (Ec), and Radiation Parameter (Ra) on Velocity profile, Temperature profile, Concentration profile, Local Skin-friction, Local Nusselt Number, plate surface temperature and Sherwood number were presented in graphically and numerically.

During the numerical computation, the Prandtl number was considered to be 0.72 which correspond to air and it is mostly encountered fluid in nature and commonly used in engineering.

The positive values of thermal Grashof number and Solutal Grashof number which are collectively referred to as buoyancy parameter correspond to the greater cooling of the surface and shows that the concentration at the plate surface is higher than the free stream concentration respectively. The cooling surface such as nuclear reactors is frequently encountered in engineering and industry. The values of Schmidt number Sc for diffusing chemical species in air were chosen to be $Sc = 0.24\ (H_2)$, $0.62\ (H_2O)$, $Sc = 0.78\ (NH_3)$ and $Sc = 2.62\ (C_9H_{12})$. Other parameters were discussed by holding $Ha = Gr = Gc = Bi = Ec = 0.1$, $Sc = 0.62$, $Pr = 0.72$, $Q = 0.01$, $Ra = 0.7$ constant for each varying parameter.

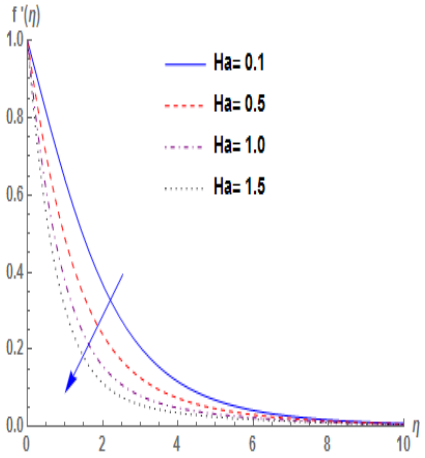

Figure 5. Velocity profile for Ha

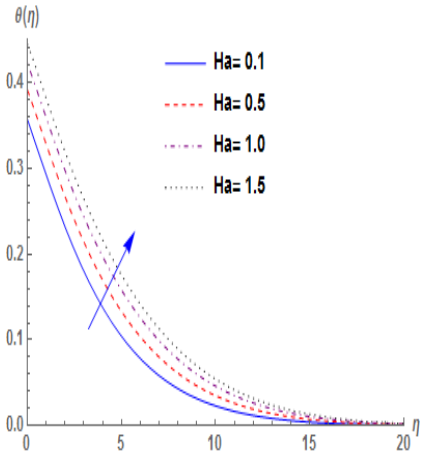

Figure 6. Temperature profile for Ha

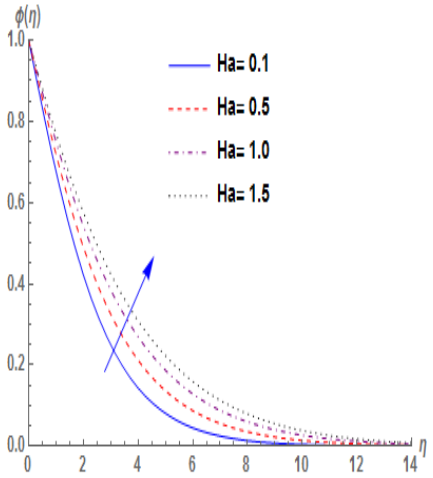

Figure 7. Concentration profile for Ha

Figure 5, 6 and 7 reveals the variation effects of Magnetic Parameter Ha, on velocity, temperature and concentration profile respectively. It is obvious from the figure 5 as expected that the velocity distribution across the boundary layer decreases with the increase in Ha. This obvious decrease is true due to the fact that increase in Magnetic field brings about an opposing force to the flow called Lorentz force which has tendency to resist motion of fluid and decrease the momentum boundary layer. However, increase in Ha as well results in frictional heating and increase the fluid temperature, magnitude of the local skin-friction, plate surface temperature and the concentration of the fluid while the Nusselt and Sherwood numbers decrease (See Fig.(6-7) and Table 2). Note that the thickness of the thermal and concentration boundary layer improve as the fluid temperature and its concentration increase.

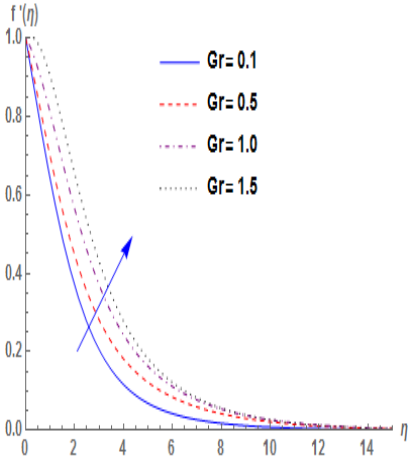

Figure 8. Velocity profile for Gr

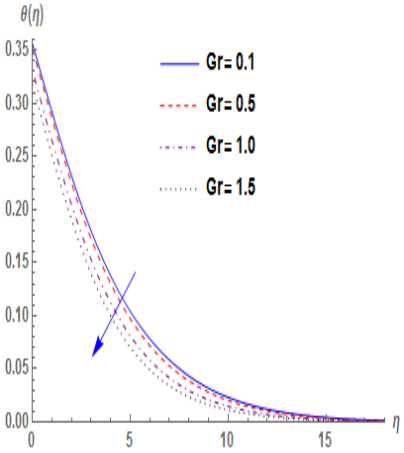

Figure 9. Temperature profile for Gr

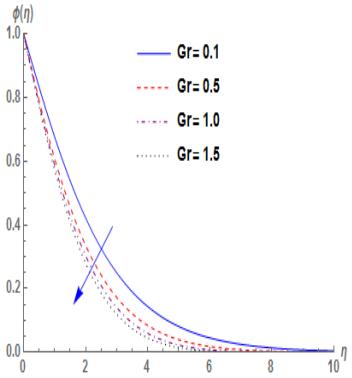

Figure 10. Concentration profile for Gr

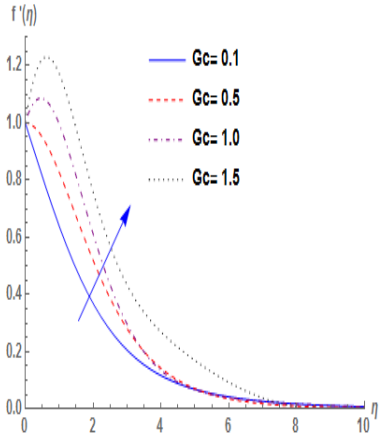

Figure 11. Velocity profile for Gc

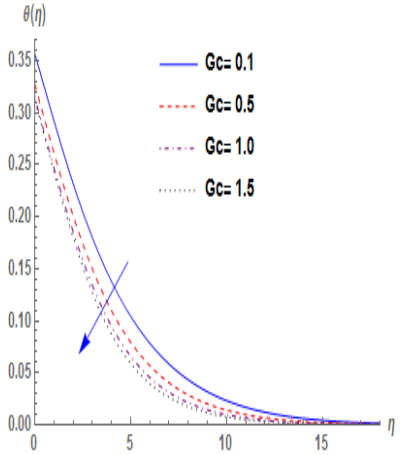

Figure 12. Temperature profile for Gc

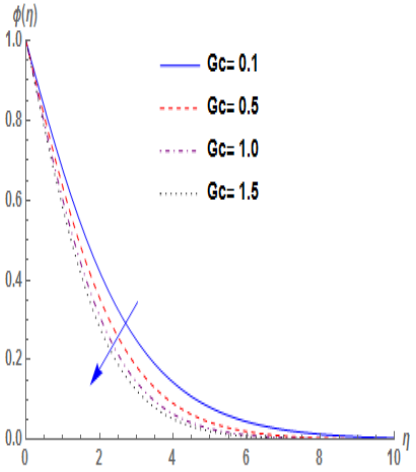

Figure 13. Concentration profile for Gc

Figures (8-13) illustrate the influence of thermal Grashof and Solutal Grashof numbers on velocity, temperature, and concentration profiles. The thermal Grashof number (Gr) signifies the relative importance of buoyancy force to the viscous hydrodynamic force within the boundary layer while the solutal Grashof number (Gc) defines the ratio of the species buoyancy force to the viscous hydrodynamic force. It can be seen from the figures 8 and 11, that increase in (Gr,Gc) gives rise to the fluid velocity within the boundary layer and suddenly fall monotonically to the free stream zero value far away from the plate surface agreeing with the far field boundary conditions which inturns increases the thickness of momentum boundary layer (See fig.8 and fig.11). It is interesting to note that the positive values of (Gr,Gc) correspond to the cooling of the plate as the fluid Temperature, Plate Surface Temperature and the fluid concentration decrease which inturns deteriorate the thickness of thermal and concentration boundary layers as shown in fig.(9-10), fig.(12-13). The Local Skin Friction, Nusselt number and Sherwood number increase with the increase in (Gr,Gc) (see table 2).

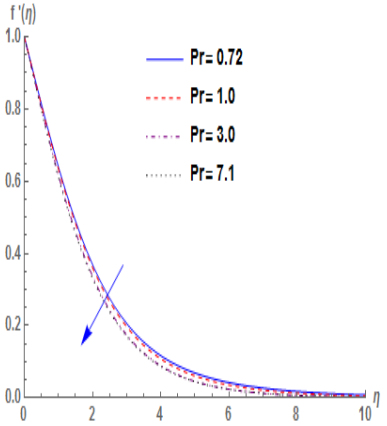

Figure 14. Velocity profile for Pr

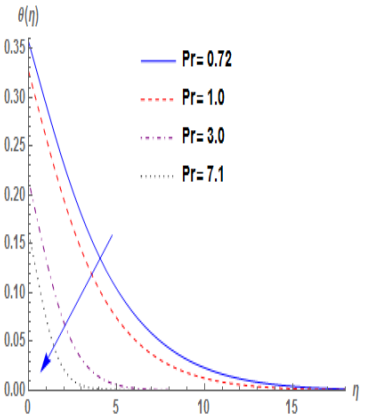

Figure 15. Temperature profile for Pr

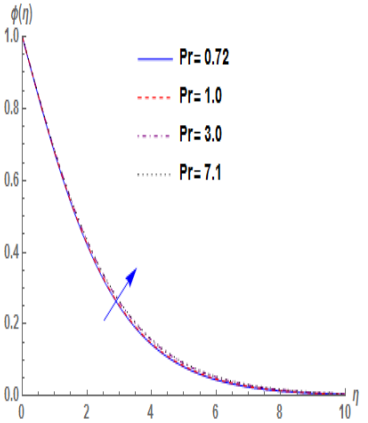

Figure 16. Concentration profile for Pr

Figures (14-16), depicts the influence of Prandtl number Pr on the velocity, temperature and concentration profiles respectively. Prandtl number Pr is a dimensionaless number, approximating the ratio of momentum diffusivity to thermal diffusivity. Increase in Pr as a result of low thermal diffusivity results in an increase in magnitude of local skin-friction, Nusselt number with a reverse phenomenon on Plate Surface Temperature and Sherwood number as shown in table 2. It can be seen from the figure that increase in Pr leads to a fall in velocity field and rapid decrease in the thermal boundary layer thickness which inturns lowers the average temperature across the boundary layer. The main reason is that, the smaller values of Pr are equivalent to increase in the thermal conductivity. This however, enable the heat to diffuse away from the heated surface more rapidly than the higher values.

Table 2. Numerical values of the Skin-friction coefficient, Local Nusselt number, Local Sherwood number and plate surface temperature

Ha	Gr	Gc	Bi	Ec	Q	Pr	Sc	Ra	$f''(0)$	$-\theta'(0)$	$\theta(0)$	$-\emptyset'(0)$
0.1	0.1	0.1	0.1	0.1	0.01	0.72	0.62	0.7	−0.370788	0.064308	0.356923	0.338928
0.5	0.1	0.1	0.1	0.1	0.01	0.72	0.62	0.7	−0.686464	0.060864	0.391360	0.294033
1.0	0.1	0.1	0.1	0.1	0.01	0.72	0.62	0.7	−0.969066	0.057813	0.421873	0.260816
0.1	0.1	0.1	0.1	0.1	0.01	0.72	0.62	0.7	−0.370788	0.064308	0.356923	0.338928
0.1	0.5	0.1	0.1	0.1	0.01	0.72	0.62	0.7	−0.188995	0.066264	0.337357	0.372221
0.1	1.0	0.1	0.1	0.1	0.01	0.72	0.62	0.7	−0.000484	0.067937	0.320633	0.402252
0.1	0.1	0.1	0.1	0.1	0.01	0.72	0.62	0.7	−0.370788	0.064308	0.356923	0.338928
0.1	0.1	0.5	0.1	0.1	0.01	0.72	0.62	0.7	−0.001613	0.067242	0.327584	0.385357
0.1	0.1	1.0	0.1	0.1	0.01	0.72	0.62	0.7	0.387627	0.068519	0.314813	0.314813
0.1	0.1	0.1	0.1	0.1	0.01	0.72	0.62	0.7	−0.370788	0.064308	0.356923	0.338928
0.1	0.1	0.1	0.5	0.1	0.01	0.72	0.62	0.7	−0.316811	0.134555	0.730889	0.350223
0.1	0.1	0.1	1.0	0.1	0.01	0.72	0.62	0.7	−0.301308	0.156786	0.843214	0.353403
0.1	0.1	0.1	0.1	0.1	0.01	0.72	0.62	0.7	−0.370788	0.064308	0.356923	0.338928
0.1	0.1	0.1	0.1	1.0	0.01	0.72	0.62	0.7	−0.347715	0.050729	0.492712	0.343464
0.1	0.1	0.1	0.1	3.0	0.01	0.72	0.62	0.7	−0.299783	0.024012	0.759877	0.353974
0.1	0.1	0.1	0.1	0.1	0.01	0.72	0.62	0.7	−0.370788	0.064308	0.356923	0.338928
0.1	0.1	0.1	0.1	0.1	0.05	0.72	0.62	0.7	−0.362516	0.060245	0.397553	0.340405
0.1	0.1	0.1	0.1	0.1	0.1	0.72	0.62	0.7	−0.348882	0.053510	0.464897	0.342695
0.1	0.1	0.1	0.1	0.1	0.01	0.72	0.62	0.7	−0.370788	0.064308	0.356923	0.338928
0.1	0.1	0.1	0.1	0.1	0.01	1.0	0.62	0.7	−0.378412	0.067350	0.326497	0.337293
0.1	0.1	0.1	0.1	0.1	0.01	3.0	0.62	0.7	−0.402666	0.078508	0.214917	0.331771
0.1	0.1	0.1	0.1	0.1	0.01	0.72	0.24	0.7	−0.332171	0.064993	0.350075	0.196666
0.1	0.1	0.1	0.1	0.1	0.01	0.72	0.62	0.7	−0.370788	0.064308	0.356923	0.338928
0.1	0.1	0.1	0.1	0.1	0.01	0.72	0.78	0.7	−0.380707	0.064110	0.358901	0.391494
0.1	0.1	0.1	0.1	0.1	0.01	0.72	0.62	0.7	−0.370788	0.064308	0.356923	0.338928
0.1	0.1	0.1	0.1	0.1	0.01	0.72	0.62	2.0	−0.383342	0.069306	0.306937	0.336197
0.1	0.1	0.1	0.1	0.1	0.01	0.72	0.62	4.0	−0.388778	0.071622	0.283778	0.334993

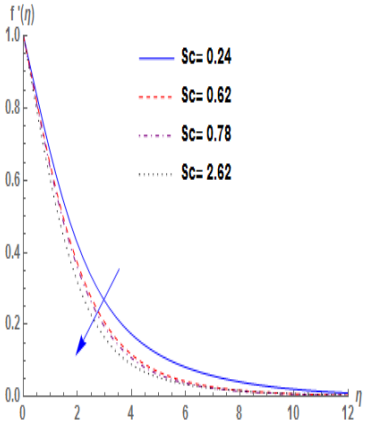

Figure 17. Velocity profile for Sc

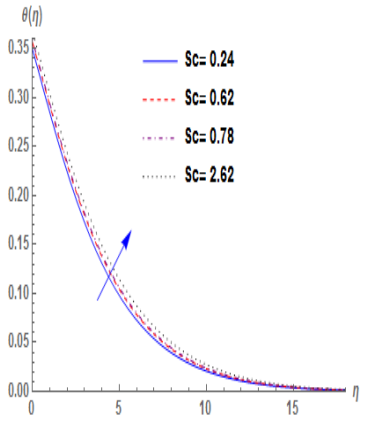

Figure 18. Temperature profile for Sc

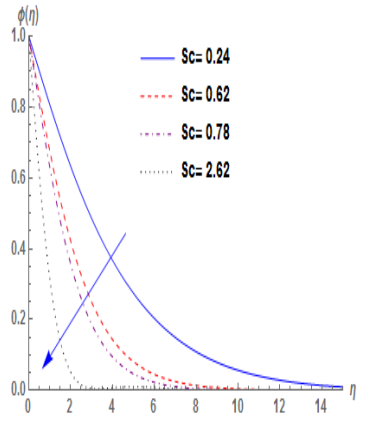

Figure 19. Concentration profile for Sc

Figures (17-19) present the effect of Schmidt number Sc, on velocity, temperature and concentration profiles. The graphical results reviews that increase in Sc, decrease the velocity distribution and concentration within the boundary layer with an improve phenomenon on fluid temperature. Also from table2, increase in Schmidt number Sc, as a result of low molecular diffusivity leads to an increase in the magnitude of Local Skin Friction, Sherwood number and Plate Surface Temperature but a decreases in Nusselt number as shown in table 2. Schmidt number measure the effectiveness of Momentum and Mass transport by diffusion in hydrodynamic boundary layers. An increase in Sc leads to a reduction in diffusion properties of the fluid and the concentration boundary layer becomes thinner than the velocity boundary layer thickness.

Figures (20-22) observe the influence of Heat Source Q on velocity, temperature and concentration profiles. As expected, the presence of heat source is to enhance the rate of heat transport to the flow which inturns overshoot the fluid temperature and increase the fluid velocity within the boundary layer while the concentration profile decrease with little effect that can hardly be seen. Moreover, the magnitude of local Skin Friction and Nusselt number decrease while Sherwood number and Plate Surface Temperature increase owning to an increasing value of Q (see table 2)

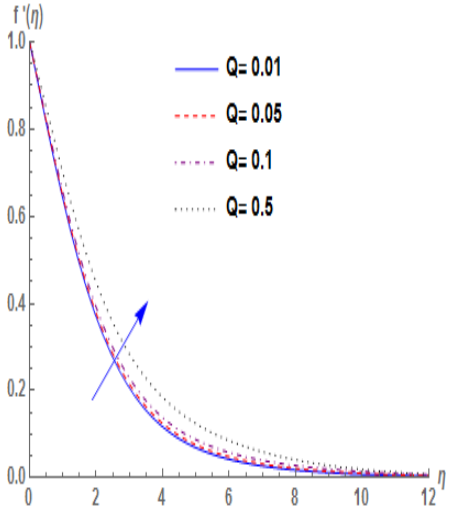

Figure 20. Velocity profile for Q

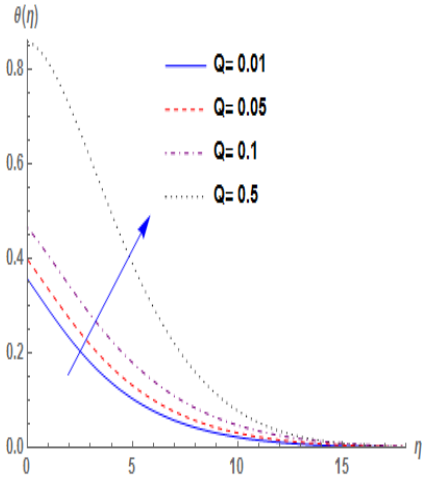

Figure 21. Temperature profile for Q

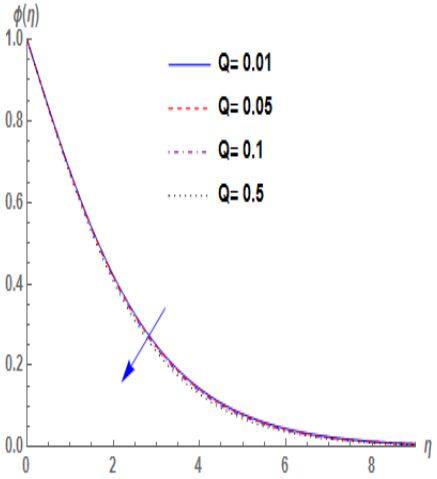

Figure 22. Concentration profile for Q

Figures (23-25) depict the effect of Eckert number on velocity, temperature and concentration profiles across the boundary layer. The Eckert number expresses the relationship between the kinetic energy of the flow and the enthalpy. As shown in table 2, the magnitude of local Skin Friction, Nusselt number decrease while the Plate Surface Temperature and the Sherwood number increase with the increase in Ec. Eckert number exhibits the conversion of kinetic energy into internal energy by work done against the viscous fluid stresses and its positive values correspond to the cooling of the plate which implies loss of heat from the plate to the fluid. However, the greater viscous dissipative heat give rise to velocity and temperature profiles but a reduction on concentration profile.

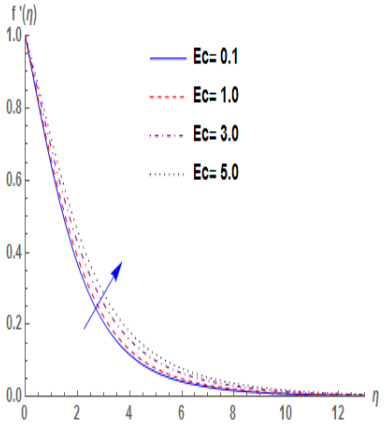

Figure 23. Velocity profile for Ec

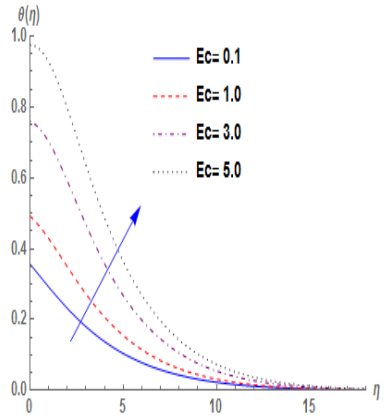

Figure 24. Temperature profile for Ec

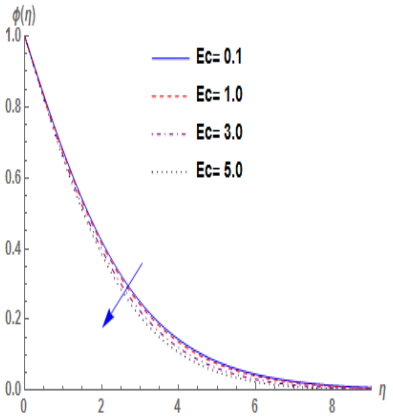

Figure 25. Concentration profile for Ec

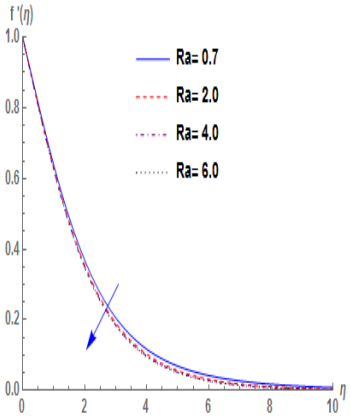

Figure 26. Velocity profile for Ra

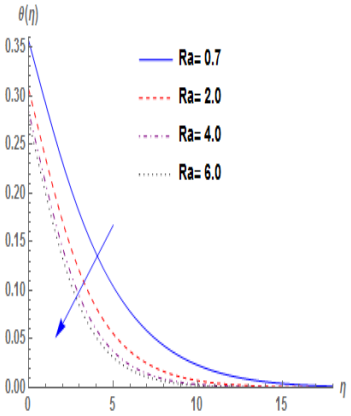

Figure 27. Temperature profile for Ra

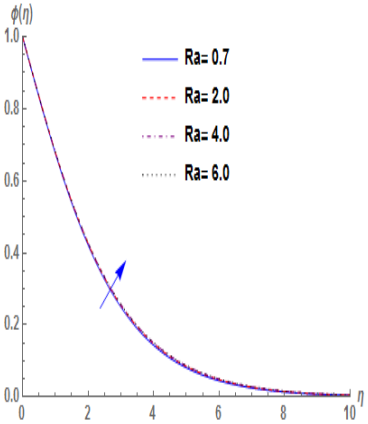

Figure 28. Concentration profile for Ra

Figures (26-28) presents the influence of Radiation Parameter Ra on velocity, temperature and concentration profiles respectively. Inflation in radiation parameter (Ra) slightly diminishes the velocity distribution with an opposite result in fluid concentration. However, the thermal condition deteriorates with the increase in Ra which in turns pioneer the decrease in thermal boundary layer thickness. This quantitatively agreed with the expectation as increase in Ra $\left(\text{See } Ra = \frac{KK^*}{4\sigma T_\infty}\right)$ contributes to the falling of radiation absorptivity K^* while the enhancement in radiative heat flux $\frac{\partial q_r}{\partial y}$ improves as K^* reduces the rate of radiative heat transfer to the fluid that consequently improve the fluid temperature. Also, increase in Ra leads to a increase in magnitude of Local Skin Friction and Nusselt number with a reverse phenomenon on Plate Surface Temperature and Sherwood number. This result is in agreement with Stanford and Sandile (2009). The effect of Thermal Radiation becomes more significant as $Ra = 0.1$ but no effect as $Ra \to \infty \; or \; Ra = \infty$.

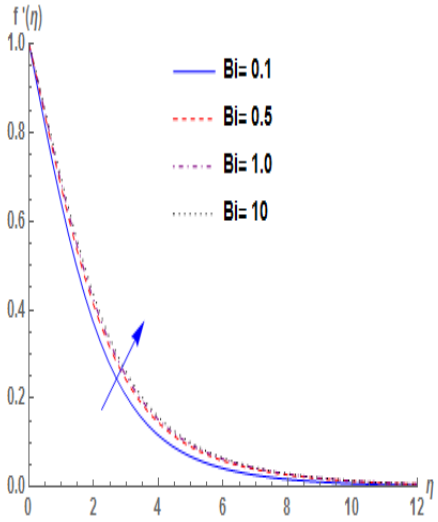

Figure 29. Velocity profile for Bi

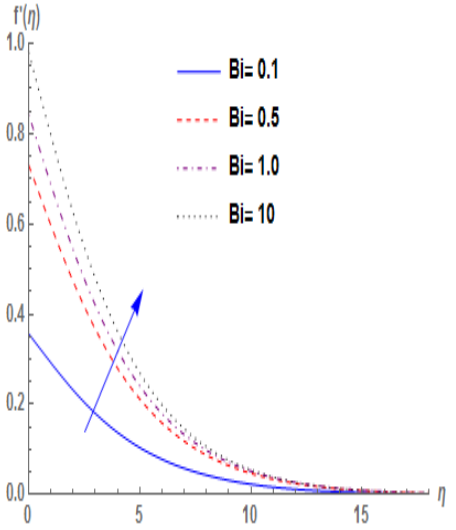

Figure 30. Temperature profile for Bi

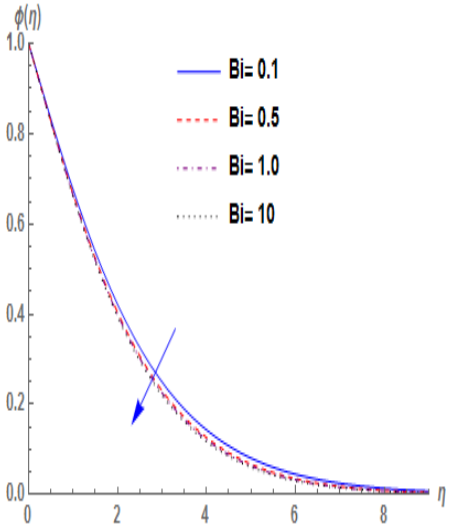

Figure 31. Concentration profile for Bi

Figures (29-31) show that the velocity and temperature profiles increases while concentration profile decreases with little effect, on the increase in the Convective Heat parameter Bi. In addition, the magnitude of Local Skin-Friction decreases while the Nusselt number, Sherwood number and Plate Surface Temperature increase on the increase in Bi as shown in table 2. This was due to the fact that the left surface of the plate is exposing to the hot fluid thereby causing the right surface to be lighter and flow faster.

6. CONCLUSION

This study has vast application in industries and engineering disciplines in understanding the dynamic flowing phenomenon which is a major language in science and technology such as cooling of nuclear reactors, cooling of electronic components and enhanced oil recovery e.t.c. In this present investigation, an analysis is made to study heat and mass transfer in hydromagnetic boundary layer flow over a moving vertical plate with convective boundary condition in the presence of thermal radiation. The resulting partial differential equations which describe the problem are transformed to dimensionless equations using Similarity method with the corresponding dimensionless variables. We then solve the equations by Homotopy Analysis Method and the results are discussed through graphs and tables for different values of embedding parameters and the following conclusion are drawn from the results obtained.

- Cooling problem is guaranteed with the positive values of (Gr, Gc) which is often encountered in engineering application such as cooling of electronic component and nuclear reactors.
- The Nusselt number increased as the values of Prandtl number, radiation parameter, and convective heat parameter increase but decrease with the increase in Schmidt number and viscous dissipation
- The momentum boundary layer thickness decrease while the thermal and concentration boundary layers thickness increase on the increase in the magnetic parameter.
- An increase in viscous dissipation parameter enhanced the velocity and temperature profiles with a reverse phenomenon on concentration profile.
- Higher values of radiation parameter Ra, pioneer the dominance of conduction over radiation and consequently depressed the thermal boundary layer thickness.

REFERENCES

[1] Das, S., Jana, R. N., and Chamkha, A. J., (2015) unsteady free convection flow past a vertical plate with heat and mass fluxes in the presence of thermal radiation. *Journal of Applied fluid mechanics., 8, 845-854.*

[2] Das. K., (2010) Extract solution of MHD free convection flow and mass transfer near a moving vertical plate in presence of thermal radiation. *African Journal of mathematical physics volume 8, 29-41*.

[3] Farooq, U., Zhao, Y. L., Hayat, T., Alsaed, A., and Liao, S. J., (2015), Application of the HAM-based Mathematica package BVPh 2.0 on MHD Falkner-skan flow of nanofluid. *www.elsevier.com/locate/compfluid*

[4] Ghara, N., Das, S., Maji, S. L., and Jana, R. N., (2012) Effect of radiation on MHD free convection flow past an impulsively moving vertical plate with ramped wall temperature. *Am. J. Sci. ind. Res. 3, 376-386.*

[5] Gnaeneswara, R. M., (2014) influence of thermal radiation, viscous dissipation, and Hall current on MHD convection flow over a stretched vertical flat plate. *Ain shams engineering journal, 5 169 – 175.*

[6] Hemalatha, E., and Bhaskar, R., (2015) Effect of thermal radiation and chemical reaction on MHD free convection flow past a moving vertical plate with a heat source and convective surface boundary condition. *Pelagia Research Advanced in Applied Science Research. 6,128-143.*

[7] Idowu A. S., Dada M. S, and Jimoh A.(2013), Heat and Mass Transfer of Magnetohydrodynamic (MHD) and dissipative fluid flow past a moving vertical porous plate with variable suction, *Mathematical theory and modeling. 3, 80-102.*

[8] Jhansi, R. K., Reddy, G. V. R., Murthy ch. V. R., and Murthy, M. V. R., (2015) heat and Mass transfer effects on MHD free convection flow over an inclined plate embedded in a porous medium. *Int. J. Chem sci: 13, 1998 – 2016.*

[9] Lakshmi, R, Jayarami, K. R., Ramakrishna, K., and Reddy, G.V. R., (2014) Numerical Solution of MHD flow over a moving vertical porous plate with heat and Mass Transfer. *Int. J.Chem. sci 12 (14), 1487 – 1499.*

[10] Liao S.J (2003), Beyond perturbation: an introduction to Homotopy Analysis Method. Boca Raton, Fla., USA: Chapman and Hall

[11] Liao SJ.(2003) On the analytic solution of magnetohydrodynamic flows of non-Newtonian fluids over a stretching sheet. *J. Fluid Mech., 488, 189–212.*

[12] Loganathan, P., Kannan, M., and Ganesan, P., (2011) Thermal Radiation effect on MHD flow over a moving semi-infinite Vertical cylinder. *Int. Journal of Math. Analysis, 5, 257 – 274.*

[13] Makinde O. D, (2010), On MHD heat and Mass Transfer over a moving vertical plate with a corrective surface boundary condition. *Can. J. Chem. Eng. 88, 983-990.*

[14] Mohammed, S. A., Mohammad, A, Md., Delowar, H. (2013) Heat and Mass transfer in MHD free convection flow over an inclined plate with hall current. *Int. J. Eng. Sci. (IJES). 2, 81 – 88.*

[15] Narahari, M., and Ishaq (2011) Radiation effect in free convection flow near a moving vertical plate with Newtonian heating. *J. Appl.Sci. 11, 1096 – 1104.*

[16] Nepal, C.R., Bishnu, P.G., and Litan, K.S., (2014), Unsteady MHD free convection flow along a vertical plate in the presence of radiative heat flux. *Applied Mathematics 4, 77-85.*

[17] Olubode, K. K., Tosin, O., Adeola, J.O., Isaac, L. A., (2016), Homotopy Analysis of MHD free Convective Micropolar Fluid Flow Along a vertical surface embedded in Non-Darcian Thermally-Stratified Medium. *Open Journal of Fluid Dynamic, 6, 198-221.*

[18] Opiyo, R. O., and Alfred, W. M., (2017), Numerical computation of steady Buoyancy Driven MHD heat and Mass Transit past an inclined infinite flat plate with sinusoidal surface Boundary conditions. *Applied Mathematical Sciences. 11, 711 – 729.*

[19] Rajput, U. S. and Kumar S. (2012) Radiation effect on MHD flow past an impulsively started vertical plate with variable heat and Mass Transfer. *Int. J. Applied Math. Mech 8, 66 – 85*.

[20] Rout, B.R.,, Parida, S.K., and Panda, S., (2013) MHD heat and mass transfer of chemical reaction fluid flow over a moving vertical plate in the presence of heat source with convective surface boundary condition. *Hindawi Publishing Corporation, Int.Jour.of chem.Eng., Art.ID 296834,10pages. http://dx.doi.org/10.1155/2013/296834*

[21] Salem A. M. and Rania, F (2012) Effect of variable properties in MHD heat and Mass transfer flow near a stagnation point towards a stretching sheet in a porous medium with thermal radiation. Chim. Phys. B. 21, 054701-054711

[22] Sandeep, N., Vijaya, B. R. A., and Sugunamma, V., (2012) Effect of Radiation and Chemical reaction on transient MHD free convective flow over a vertical plate through porous media. Chem. and process. Eng. Research. 2, 1-9

[23] Seethamahalakshmi, Reddy, G. V. R., and Prasad, B. D. C. N., (2011), Unsteady MHD free convection flow and mass transfer near a moving vertical plate in the presence of thermal radiation. Advance in Applied Science Research, 2, 261-269

[24] Siva, R. S., Ali, J. C., and Anjan, K. S., (2016), Heat and mass transfer effects on MHD natural convection flow past an impulsively moving vertical plate with ramped temperature. American Journal of heat and mass transfer. 3,129-148

[25] Stanford, S., and Sandile, S. M., (2009), Thermal Radiation effects on Heat and Mass transfer over an unsteady stretching surface. Mathematical Problem in Engineering, Hindawi Pub. Corp. ID965603, *doi:10.1155/2009/965603.*